Proceedings of the
44th IEEE Conference on Decision and Control, and
the European Control Conference 2005
Seville, Spain, December 12-15, 2005

MoB15.2

PPF Control of a Piezoelectric Tube Scanner

(Invited Paper)

M. Ratnam, B. Bhikkaji, A. J. Fleming and S. O. R. Moheimani

Abstract— Piezoelectric tubes are commonly used in Scanning Tunnelling Microscopes and Atomic Force Microscopes to scan material surfaces. In general, scanning using a piezoelectric tube is hampered by the presence of low-frequency mechanical modes that are easily excited to produce unwanted vibration. In this work, a Positive Position Feedback controller is designed to mitigate the undesired mechanical resonance. Experimental results reveal a significant damping of the mechanical dynamics, and consequently, an improvement in tracking performance.

I. INTRODUCTION

Scanning Tunneling Microscopes (STM) and Atomic Force Microscopes (AFM) were developed in the 1980's by Binnig, Quate and Gerber, see [1] and [2]. STMs are capable of imaging the topography of conducting material surfaces at atomic resolution, while AFMs are capable of imaging arbitrary surfaces with submicron resolution. In both STMs and AFMs, a probe is placed in close proximity, typically a few Angstroms, to the surface for which a topographic map is desired. The given surface is scanned by either moving the probe, or the sample surface, so that the scanning head interacts with the entire region of interest. The physical unit in the STM, or the AFM, that regulates the motion of the probe, or the surface, is referred to as the *scanning system*.

In general, scanning in both SPMs and AFMs is done by attaching the probe to a piezoelectric tube or placing the sample on the top of a piezoelectric tube, and actuating the piezoelectric tube in a raster pattern, see [3], [4] and [5].

One of the advantages of using piezoelectric tubes for scanning is that their dynamics can be well approximated by linear models, see [3], [4], [5], [6], [7] and [8]. However, these linear models normally possess lightly damped mechanical modes. In other words, piezoelectric tubes are susceptible to mechanical vibrations. Further non-linearities such as creep and hysteresis are also present, when actuating the tube with low frequency inputs (near DC signals) and high voltage inputs respectively. The presence of mechanical vibrations and the non-linearities hinder the actuation of the tube.

In this paper a piezoelectric tube is considered. A linear model is constructed for the piezoelectric tube using standard system identification techniques [9], [10] and [11]. The resonance peak of interest is damped by designing a suitable Positive Position Feedback controller. The resulting scanning system, a piezoelectric tube with the PPF controller, is

The authors are with the School of Electrical Engineering and Computer Science, University of Newcastle, NSW 2308, Australia. R. Moheimani is the corresponding author. Reza.Moheimani@newcastle.edu.au

actuated to follow a raster pattern smoothly. As a note of caution, non-linearities such as creep and hysteresis have been avoided by choosing scanning signals that do not have low frequency components and high voltages amplitudes.

Positive Position Feedback (PPF) is a control technique introduced by Caughey, Fanson and Goh, see [12] and [13] to suppress the mechanical vibrations in a structure. In the past some authors have successfully used the PPF controller in different contexts, see [14], [15], [16] and [17]. Here, a PPF controller is designed to damp the vibrations in a piezoelectric tube scanner, and it is shown that good damping can be achieved by using these controllers. To the best of the authors knowledge, no research papers where PPF controllers have been used for damping vibrations in piezoelectric tube scanners have yet been published.

In this paper, some new approaches have been presented for controlling the piezoelectric tube scanner. Firstly, the inbuilt transducers in the piezoelectric tube are used as both sensors and actuators. Here, a pair of piezoelectric patches in the tube are used as actuators and their collocated counterparts are used as sensors. In relatively high bandwidth applications, collocated sensor electrodes are superior to external sensors as their resolution and bandwidth are greater. In addition, external noises, which are typical of external sensors, are not as significant when using inbuilt sensors. Nevertheless, it has been a common practice to use external sensors in piezoelectric tube scanning, see [3] and [4]. Secondly, as mentioned above, a PPF controller is used to remove structural vibrations resulting from the first mechanical resonance mode, and with good results. The PPF controller due to its structure enables more accurate and higher frequency actuation. Finally, the design of the experimental setup is open for extensions, including extending the models to compensate for creep, as well as implementing a charge rather than voltage control to compensate for hysteresis.

II. SYSTEM DESCRIPTION

A piezoelectric tube scanner normally consists of a thin-walled cylindrical tube of a piezoelectric material with a thin coating of copper or silver in its inner and outer walls, see Figure 1. The copper coating on the inner and outer walls of the piezoelectric tube acts as the scanner electrodes. The outer electrode is axially quartered into four equal sections. Conventionally, a pair of the opposite sections of the quartered electrode is referred to as the $x-x$ electrodes, and the other pair is referred to as the $y-y$ electrodes.

In order to model and actuate the piezoelectric tube scanner, an experimental setup was devised as follows: a device

Fig. 1.   Piezoelectric Tube

Fig. 3.   Input-Output Diagram
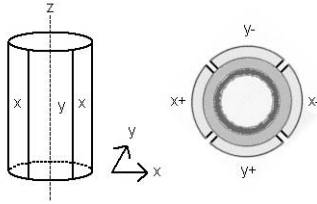
was constructed to hold the piezoelectric tube along the z axis with the lower end of the tube facing a large aluminium block. A small aluminium cube is bonded to the upper end of the tube. The head of a ADE Technologies 4810 capacitive sensor is placed in close proximity to the aluminium cube. The inner electrode of the piezoelectric tube is grounded. One electrode of each of the $x - x$ and $y - y$ pairs, referred to as x^+ and y^+ respectively, are chosen as the input ends of the piezoelectric tube, and the corresponding opposite ends, referred to as x^- and y^- respectively, are chosen as the output ends of the piezoelectric tube. A schematic description of the experimental setup is shown in Figure 2.
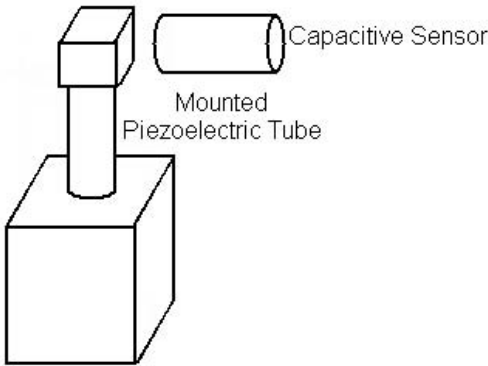

Fig. 2.   Schematic Diagram

When input voltage signals V_{x+} and V_{y+} are applied to the x^+ and y^+ electrodes respectively, the piezoelectric tube deforms. This deformation changes the voltages V_{x-} and V_{y-} measured at the output electrodes x^- and y^-. Furthermore, due to the deformation of the tube, the capacitance between the aluminium cube and the head of the capacitive sensor changes. This change in the capacitance, C, is also recorded as an output. In total, the given piezoelectric tube scanner is interpreted as a linear system with two inputs, $\begin{bmatrix} V_{x+}, V_{y+} \end{bmatrix}^\top$ and three outputs $\begin{bmatrix} V_{x-}, V_{y-}, C \end{bmatrix}^\top$, see Figure 3. However, in all the experiments to be performed here, for both modelling and actuating the piezoelectric tube, only the outputs $\begin{bmatrix} V_{x-}, V_{y-} \end{bmatrix}^\top$ will be used. The third output, C, will be used as an indicator of the lateral displacements of the tube along the x direction from its original position.
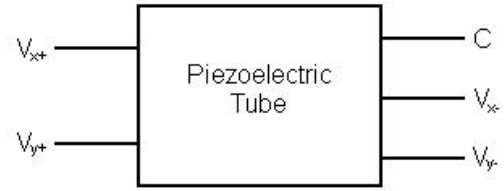
III. OPEN LOOP CONTROL

As mentioned earlier the goal of this paper is to actuate the piezoelectric tube in a raster pattern. Therefore a desired path of the piezoelectric tube would be to repeatedly trace straight lines back and forth in x direction, while slowly increasing its position in the y direction. A common practice to achieve such a path is to input a triangle wave in x^+ electrode and a "very slowly" increasing ramp in the y^+ electrode as reference signals for the system. Infact, to have a good scan of the surface the changes in y direction must be "quasi-static" with respect to the changes in the x direction. Normally in most cases the slowly varying ramp in the y^+ electrode is either replaced by a dc signal or assumed to be earthed, see [3], [4] and [18].

In Figure 4, we have plotted the response (output) C recorded by the capacitive sensor to a triangle wave input of 6V and 81Hz at the x^+ electrode with the y^+ electrode being earthed. Note that the capacitive sensor output does not exactly match the triangle wave input, but appears to be equal to the triangle wave input plus certain periodic corrugations. This implies that the lateral displacement of the tube along the x direction is not really a straight line but rather a highly corrugated straight line. The distortion in the capacitive sensor output is due to the amplification of harmonics of the triangle wave that are close to the resonance frequencies of the piezoelectric tube, in particular, the first resonance mode when applying this input signal. Hence, damping these resonances in the piezoelectric tube would effectively suppress the amplification of these harmonics.

IV. SYSTEM IDENTIFICATION

In this section, the transfer function $G_{xx}(s)$ relating the input at x^+ electrode and the output at x^- electrode is modelled using standard techniques of system identification.

System identification is an experimental approach to the modelling of dynamic systems, see [9], [10] and [11]. An experiment is performed by exciting the system with known inputs and recording the corresponding outputs. A model is then designed for the recorded input-output data.

Here, an experiment was performed on the piezoelectric tube by inputting swept sine waves into the electrode x^+,
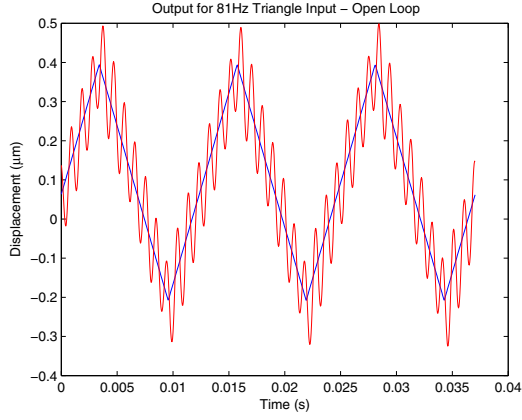
Fig. 4. Response recorded by capacitive sensor

with y^+ electrode being earthed, and recording the corresponding output at x^-, using a HP 35670A dual channel Spectrum Analyser. The Spectrum Analyser was also used to process the recorded input output data and obtain the non-parametric frequency response function (FRF), $G_{xx}(i\omega)$, corresponding to the transfer function $G_{xx}(s)$. In Figure 5 the non-parametric FRF $G_{xx}(i\omega)$ obtained from the Spectrum Analyser is plotted. It can be inferred from Figure 5 that the piezoelectric tube has a strong resonant behaviour around $1000 - 1100$Hz frequency. And from the phase plot it is fairly evident that second order models could give good fits to the plotted non-parametric data. The following second order model was found to fit the non-parametric data

$$G_{xx}(s) = \frac{1.841 \times 10^7}{s^2 + 88.77s + 4.33 \times 10^7} - 0.1884 \quad (1)$$

In Figure 5 the parametric fit of $G_{xx}(i\omega)$, see (1), is plotted along with the non-parametric data. It can be inferred that the parametric model fits the non-parametric data reasonably well. Details on how the models were estimated are not presented here as the models are of low order and their estimation is rather straightforward.
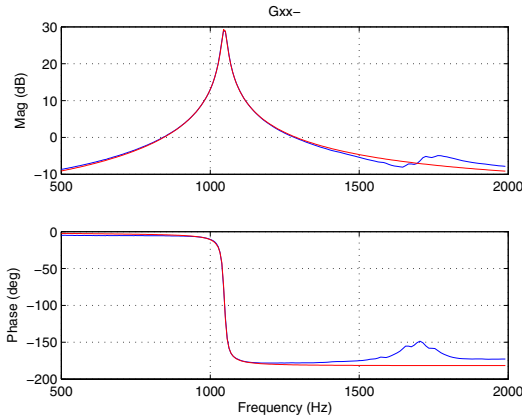

Fig. 5. Bode magnitude plots of the non-parametric model (blue) along with their corresponding parametric models (red).

V. PPF CONTROLLER

Positive Position Feedback (PPF) is a control technique meant to suppress the vibrations in second order systems. As its name suggests, the output of a second order system is positively fed back into the system through a controller. This approach was first introduced in [12] and [13] for scalar second order systems. PPF was used in a multivariable form in [19] to suppress the mechanical vibrations in a cantilever beam. In this paper, the PPF controller is considered in its original form, as in [12] and [13], and a suitable design scheme is presented to suppress the resonance peak in $G_{xx}(i\omega)$.

A PPF controller for one vibration mode is a second order system with a transfer function of the form

$$K_{PPF}(s) = \frac{\omega_p^2}{s^2 + 2\eta_p\omega_p s + \omega_p^2}, \quad (2)$$

where ω_p and η_p are the design variables. Here, the output of the x^- electrode is positively fed back into the input electrode x^+ through the PPF controller K_{PPF}, (2), see Figure 6. It can be checked that the input-output relation
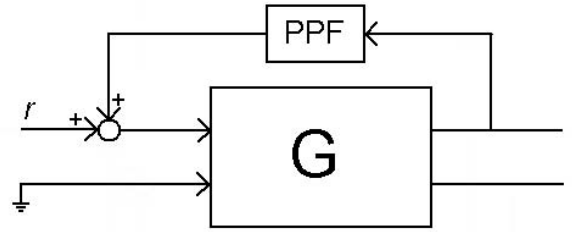

Fig. 6. Closed-loop system

between the reference signal r and the output signal V_{x^-} in the closed-loop system, Figure 6, is given by

$$V_x^- = \frac{G_{xx}}{1 - G_{xx}(s)K_{PPF}(s)}r,$$
$$\triangleq G_{CL_x}(s)r. \quad (3)$$

Adhering to the notations in [12] and [13], the transfer function $G_{xx}(s)$ is rewritten as

$$G_{xx}(s) = \frac{g\omega_0^2}{s^2 + 2\eta_0\omega_0 s + \omega_0^2} + D, \quad (4)$$

where

$$g = 0.4252 \quad (5)$$
$$\eta_0 = 0.0067 \quad (6)$$
$$D = -0.1884 \quad (7)$$

and

$$\omega_0 = 6580.3 \text{ rads/sec.} \quad (8)$$

The design parameters η_p and ω_p of the PPF controller (2), are chosen such that the magnitude response of $G_{CL_x}(s)$, (3), is more damped when compared with the magnitude response of (4).

In order to motivate the idea behind the design scheme, consider the FRF of the system (4)

$$G_{xx}(\mathrm{i}\omega) = \frac{g\omega_0^2}{\omega_0^2 - \omega^2 + \mathrm{i}2\eta_0\omega_0\omega} + D. \qquad (9)$$

As the damping coefficient η_0 is "approximately" zero, at the resonance frequency ω_0, the magnitude response $\mid G_{xx}(\mathrm{i}\omega_0) \mid$ (the resonance peak) takes a large value, see Figure 5. It is known that second order systems with $\eta_0 > \frac{1}{2}$ do not have any distinguishable resonance peaks. The reason for having a huge resonance peak at ω_0 in Figure 5 is that the real part of the denominator of (9) is zero and the imaginary part is "very small". For a well damped system, with $\eta_0 > \frac{1}{2}$, only the real part is zero, whereas the imaginary part is "quite large", thereby having a lower magnitude at ω_0. In the PPF design scheme to be presented here, the PPF parameters η_p and ω_p are chosen such that the FRF $G_{CL_x}(\mathrm{i}\omega)$ has a denominator which is "large" for all frequency points.

In the design scheme, for both technical ease and to have conciseness in expressions, the given system (4) is approximated by a pure resonance system. This approximation is valid as the damping coefficient η_0 is indeed approximately zero and the feedthrough term D is very small when compared with the magnitude of the resonance peak $\mid G_{xx}(\mathrm{i}\omega_0) \mid$. Introduction of the approximation $\eta_0 = D = 0$ leads to

$$
\begin{aligned}
G_{CL_x}(s) &= \frac{\frac{g\omega_0^2}{s^2+\omega_0^2}}{1 - \frac{g\omega_0^2\omega_p^2}{(s^2+\omega_0^2)(s^2+2\eta_p\omega_p s+\omega_p^2)}} \\
&= \frac{g\omega_0^2(s^2 + 2\eta_p\omega_p + \omega_p^2)}{(s^2 + \omega_0^2)(s^2 + 2\eta_p\omega_p s + \omega_p^2) - g\omega_0^2\omega_p^2}, \\
&\triangleq \frac{N(s)}{D(s)}.
\end{aligned}
\qquad (10)
$$

This implies

$$G_{CL_x}(\mathrm{i}\omega) = \frac{N(\mathrm{i}\omega)}{D(\mathrm{i}\omega)}, \qquad (11)$$

where

$$N(\mathrm{i}\omega) = g\omega_0^2(\omega_p^2 - \omega^2 + 2\mathrm{i}\eta_p\omega_p\omega) \qquad (12)$$

and

$$
\begin{aligned}
D(\mathrm{i}\omega) &= (\omega^4 - (\omega_0^2 + \omega_p^2)\omega^2 + \omega_p^2\omega_0^2(1 - g)) \\
&- \mathrm{i}2\eta_p\omega_p\omega(\omega^2 - \omega_0^2) \\
&\triangleq D_R(\mathrm{i}\omega) + \mathrm{i}D_I(\mathrm{i}\omega).
\end{aligned}
\qquad (13)
$$

For the closed-loop system not to have distinguishable resonance peaks, $\mid D(\mathrm{i}\omega) \mid$ must never be "close to zero" for all frequencies ω. In particular, for the frequency points where the real part $D_R(\mathrm{i}\omega)$ is zero, or "close to zero", the imaginary part $D_I(\mathrm{i}\omega)$ must be "large or away from zero", and vice versa.

It can be checked that the biquadratic term $D_R(\mathrm{i}\omega)$, (13), has roots at

$$\omega_{r1}^\pm = \pm\sqrt{\frac{1}{2}(\omega_0^2 + \omega_p^2 + \sqrt{(\omega_0^2 - \omega_p^2)^2 + 4g\omega_0^2\omega_p^2})} \qquad (14)$$

and

$$\omega_{r2}^\pm = \pm\sqrt{\frac{1}{2}(\omega_0^2 + \omega_p^2 - \sqrt{(\omega_0^2 - \omega_p^2)^2 + 4g\omega_0^2\omega_p^2})}, \qquad (15)$$

and has three saddle points at $\omega = 0$ and

$$\omega_s^\pm = \pm\sqrt{\frac{\omega_0^2 + \omega_p^2}{2}}. \qquad (16)$$

Similarly it can be checked that the imaginary part $D_I(\mathrm{i}\omega)$ is an odd function with roots $\pm\omega_0$ and 0, and has two saddle points at $\pm\frac{\omega_0}{\sqrt{3}}$. It is also worth noting that roots of $D_R(\mathrm{i}\omega)$ and $D_I(\mathrm{i}\omega)$ interlace each other, *i.e.,*

$$\omega_{r1}^+ > \omega_0 > \omega_{r2}^+ > 0 > \omega_{r2}^- > -\omega_0 > \omega_{r1}^-, \qquad (17)$$

which is a necessary and sufficient condition for stability.

If ω_p were to be chosen such that $\omega_p \ll \omega_0$, it can be directly inferred from (14) and (15) that

$$\omega_{r1}^\pm \approx \pm\omega_0 \qquad (18)$$

and

$$\omega_{r2}^\pm \approx 0. \qquad (19)$$

In other words, for choices of ω_p much smaller than ω_0 the zeros of $D_R(\mathrm{i}\omega)$ would be approximately equal to the zeros of $D_I(\mathrm{i}\omega)$, which as a consequence would lead to sharp resonance peaks around the frequency points $\pm\omega_0$ and 0 in the magnitude plot of $G_{CL_x}(\mathrm{i}\omega)$. Alternatively, if ω_p were to be chosen such that $\omega_p \gg \omega_0$, then, as before, it can be verified from (14) and (15) that

$$\omega_{r1}^\pm \approx \pm\omega_p \qquad (20)$$

and

$$\omega_{r2}^\pm \approx 0. \qquad (21)$$

It is apparent from (21) that for choices of ω_p much larger than ω_0, the magnitude response would have large resonance peaks around $\omega = 0$. The above observations for large and small choices of ω_p were reported in [14] and [15], however no clear reasoning for this behaviour was provided therein.

A simple and effective option to keep the zeros of $D_R(\mathrm{i}\omega)$ and $D_I(\mathrm{i}\omega)$ apart, is to match zeros of $D_I(\mathrm{i}\omega)$ with the saddle points of $D_R(\mathrm{i}\omega)$, *i.e.,* let

$$\sqrt{\frac{\omega_0^2 + \omega_p^2}{2}} = \omega_0, \qquad (22)$$

which implies,

$$\omega_p = \omega_0. \qquad (23)$$

Choosing $\omega_p = \omega_0$ may not be the best choice but certainly a prudent one. Another alternative is to plot the graphs of $D_R(\mathrm{i}\omega)$ and $D_I(\mathrm{i}\omega)$ plots, with $\omega_p = \alpha\omega_0$, for several values of α, for example setting $\alpha = 0.5k, \ k = 1, 2, 3, \ldots,$ and manually inspecting the "closeness" of the zeros of $D_R(\mathrm{i}\omega)$ and $D_I(\mathrm{i}\omega)$ for each α. Note that in the current context this is not a difficult task as changing ω_p only scales $D_I(\mathrm{i}\omega)$ and has no effect on its roots. Hence a manual

verification of the closeness of the zeros of $D_R(i\omega)$ and $D_I(i\omega)$ effectively involves comparing one plot of $D_I(i\omega)$ with many plots of $D_R(i\omega)$. In this paper we have set $\omega_p = \omega_0$ and $\eta_p = 0.56$. The plots of $D_R(i\omega)$ and $D_I(i\omega)$ with $\omega_p = \omega_0$ and $\eta_p = 0.56$ are shown in Figure 7. Notice that the roots of $D_R(i\omega)$ and $D_I(i\omega)$ are reasonably further apart and the saddle points of $D_R(i\omega)$ match the zeros of $D_I(i\omega)$. This avoids a resonance peak in the closed-loop transfer function $G_{CL_x}(i\omega)$, see Figure 8. Figure 8 suggests a 30dB damping in the magnitude of $G_{CL_x}(i\omega)$ around the resonance frequency ω_0. Even though theortically, such a damping can be achieved using traditional controllers like Lead-Lag, LQG and other traditional controllers, the control effort required and the complexity involved in implementing them would be significantly higher, see [3], [4], [5] and [20].
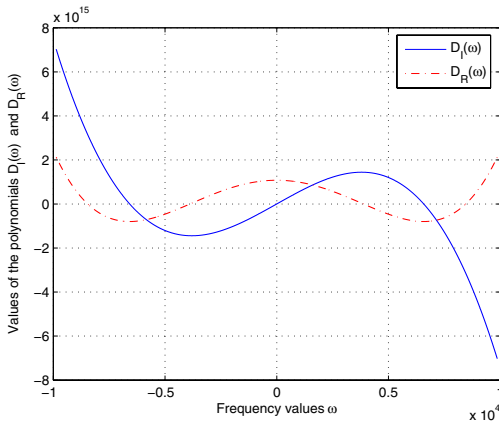

Fig. 9.   Response recorded by capacitive sensor for the closed-loop system.

Fig. 7.   Plots of the polynomials $D_R(\omega)$ and $D_I(\omega)$ with $\omega_p = \omega_0$ and $\eta_p = 0.56$.
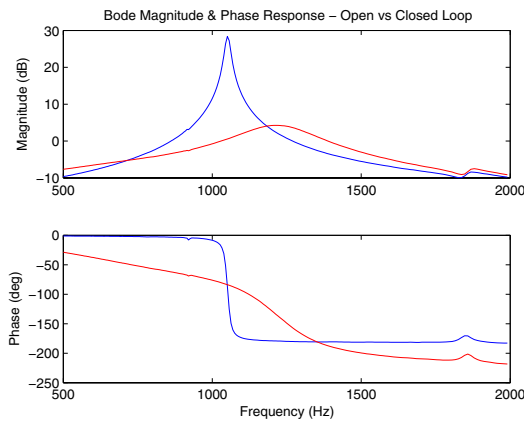

Fig. 8.   Bode plots of the transfer function $G_{CL_x}(i\omega)$.

In Figure 9 we have plotted the response of the closed-loop system, the piezoelectric tube with PPF controller as described in Figure 6, to the same triangle wave input of 81 Hz. Note that the closed loop system tracks the triangle wave more smoothly.
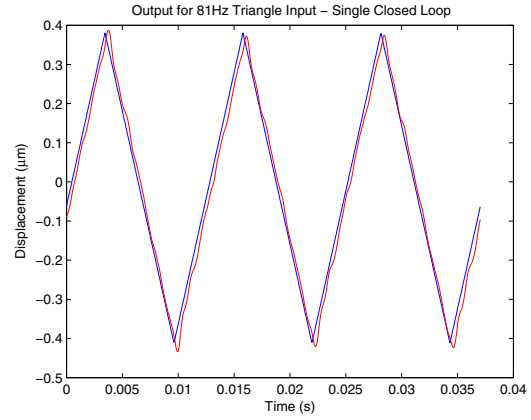
VI. CONCLUDING DISCUSSION

The tracking performance of piezoelectric tube scanners is heavily degraded by the presence of low-frequency resonant mechanical modes. Components of the reference signal and external noise near-in-frequency to the mechanical resonance are significantly amplified.

By utilizing a scanner electrode as a sensor, this paper introduces a simple voltage feedback technique for the mitigation of mechanical resonance. The PPF class of controllers is shown to provide a significant increase in the effective modal damping. The first mechanical mode of an experimental tube scanner is successfully attenuated by greater than 25 dB in one dimension. Consequently, tracking performance is significantly improved.

Although piezoelectric hysteresis was not evident in this work due to low drive voltages, it has been cited as the foremost difficulty associated with piezoelectric tube scanners. In future work, we propose the inclusion of a charge amplifier to provide immunity to piezoelectric hysteresis. An extension to two dimensions is also a high priority.

REFERENCES

[1] G. Binning, C. F. Quate and C.Gerber, "Atomic Force Microscopes", *Phys. Rev. Lett.*, vol. 56, no. 9, 1986, pp 930-933.
[2] G. Binning, H. Roher, C.Gerber and E. Weibel, "Scanning Tunneling Microscopes", *Phys. Rev. Lett.*, vol. 49, 1982, pp 57
[3] N. Tamer and M. Daleh, "Feedback Control of Piezoelectric Tube Scanners", *in Proc. of the 33rd Conference on Decision and Control*, Lake Buena Vista, Florida, 1994, pp. 1826-1831.
[4] A. Daniele, S. Salapaka, M. V. Salapaka and M. Daleh, "Piezoelectric Tubes for Atomic Force Microscopes: Design of Lateral Sensors, Identification and Control", *in Proc. of the American Control Conference*, San Diego, California, 1999, pp. 253-257.
[5] S. Salapaka and A. Sebastian, "Control of Nanopositioning Devices", *in Proc. of the 42nd IEEE Conference on Decision and Control*, Maui, Hawaii, 2003, pp. 2644-2648.
[6] M. E. Taylor, "Dynamics of Piezoelectric Tube Scanners for Scanning Probe Microscopy", *Rev. Sci. Instruments*, vol. 64(1), 1993, pp 154-158.
[7] O. M. El Rifai and K. Youcef-Toumi, "Coupling of Piezoelectric Tube Scanning in Scanning Probe Microscopes", *in Proc. of the American Control Conference*, Arlington, Virginia, 2001, pp 3251-3255.
[8] T. Ohara and K. Youcef-Toumi, "Dynamics and Control of Piezo Tube Actuators for Subnanometer Precision Applications" *in Proc. of the American Control Conference*, Seattle, Washington, 1995, pp 3308-3312.

[9] T. Soderstrom and P. Stoica, "System Identification", 1989, Prenctice-Hall, Englewood Cliffs, NJ.

[10] L. Ljung, "System Identification: Theory for the user", 1999, Prentice-Hall, Upper Saddle River , NJ.

[11] R. Pintelon and J. Schoukens, "System Identification: A Frequency Domain Approach", 2001, IEEE press , New York.

[12] J. L. Fanson and T. K. Caughey, "Positive Position Feedback Control for Large Space Structures", *AIAA Journal*, Vol 28 (4), 1990, pp 717-724.

[13] T. K. Caughey and C. J. Goh. "Analysis and Control of Quasi Distributed Parameter Systems", 1982, California Inst. of Technology, Pasadena, CA, Dynamics Lab. Rept, DYNL-82-3.

[14] G. Song and B. N. Agrawal, "Vibration Suppression of Flexible Spacecraft During Attitude Control", *Acta Astonautica*, Vol 49 (2), 2001, 73-83

[15] G. Song, S. Schmidt and B. N. Agrawal, "Experimental Study of Vibration Suppression of Flexible Spacecraft using Modular Control Patch ", *Porc. of IEEE Aerospace Conference*, Snowmass, Colarado, 1998.

[16] C. Choi and K. Park, "Self-Sensing Magnetic Levitation using LC Resonant Circuit", *Sensors and Actuators*, 1999, pp 169-177.

[17] J. J. Dosch, D. J. Leo and D. J. Inman, "Comparison of Vibration Control Schemes for a Smart Antenna", *in Proc. of the 31st Conference on Decision and Control*, Tucson, Arizona, 1992, pp. 1815-1820.

[18] G. Schitter and A. Stemmer, "Identification and Open-Loop Tracking Control of a Piezoelectric Tube Scanner for High-Speed Scanning Probe Microscopy", *IEEE Transactions on Control Systems Technology*, Vol 12 (3), 2003, pp 449-454.

[19] S.O.R. Moheimani, B. J. G. Vautier and B. Bhikkaji, "Experimental Implementation of Extended Multivariable PPF Control on an Active Structure", *submitted for publication in Proc. of the 44th IEEE Conference on Decision and Control*, Seville, Spain, 2005.

[20] K. K. Denoyer and M. K. Kwak, "Dynamic Modelling and Vibration Suppression of a Slewing Structure Utilizing Piezoelectric Sensors and Actuators", *Journal of Sound and Vibration*, Vol. 189, 1996, 13-31.